

DESY 00-067

hep-ph/0004228

April 2000

**Next-to-leading Order Calculation of the
Color-Octet 3S_1 Gluon Fragmentation Function
for Heavy Quarkonium**

Eric Braaten

Physics Department, Ohio State University, Columbus OH 43210, USA

Jungil Lee

II. Institut für Theoretische Physik, Universität Hamburg, 22761 Hamburg, Germany

Abstract

The short-distance coefficients for the color-octet 3S_1 term in the fragmentation function for a gluon to split into heavy quarkonium states is calculated to order α_s^2 . The gauge-invariant definition of the fragmentation function by Collins and Soper is employed. Ultraviolet divergences are removed using the $\overline{\text{MS}}$ renormalization procedure. The longitudinal term in the fragmentation function agrees with a previous calculation by Beneke and Rothstein. The next-to-leading order correction to the transverse term disagrees with a previous calculation.

Typeset using REVTeX

I. INTRODUCTION

The cross sections for heavy quarkonium states probe the production of heavy-quark-antiquark pairs with small relative momenta. Many of the theoretical uncertainties in quarkonium production decrease at large transverse momentum. Factorization theorems for inclusive single-hadron production [1] guarantee that the dominant mechanism for producing heavy quarkonia with high p_T is fragmentation [2], the production of a parton which subsequently decays into the quarkonium state and other partons. This process is described by a fragmentation function $D(z, \mu)$, where z is the longitudinal momentum fraction of the quarkonium state and μ is a factorization scale.

The NRQCD factorization formalism [3] can be used to factor the fragmentation functions $D(z, \mu)$ for quarkonium into NRQCD matrix elements, which can be regarded as phenomenological parameters, and short-distance factors, which depend on z and are calculable in perturbation theory. Most of the phenomenologically relevant short-distance factors begin at order α_s^2 and have been calculated to leading order. However there is one short-distance factor that begins at order α_s . It is the color-octet 3S_1 term in the gluon fragmentation function, whose NRQCD matrix element is denoted $\langle O_8({}^3S_1) \rangle$. This term is of particular phenomenological importance. Braaten and Yuan showed that it must be included in the gluon fragmentation function for triplet P-wave states in order to avoid an infrared divergence in the short-distance coefficient of the color-singlet matrix element $\langle O_1({}^3P_J) \rangle$ [4]. Braaten and Fleming argued that the $\langle O_8({}^3S_1) \rangle$ term is also phenomenologically necessary in the gluon fragmentation function for spin-triplet S-wave states in order to explain the production rate of direct J/ψ and ψ' at large p_T at the Tevatron [5]. This led to the remarkable prediction by Cho and Wise that J/ψ and ψ' at large p_T should be transversely polarized [6].

In the earliest calculations of fragmentation functions for heavy quarkonium [2,7,8], the short-distance factors were deduced by comparing the cross sections for quarkonium production with the form predicted by the factorization theorems for inclusive single-hadron

production. However the fragmentation functions can also be defined formally as matrix elements of bilocal operators in a light-cone gauge [9] or, more generally, as matrix elements of non-local gauge-invariant operators [1]. The gauge-invariant definition of Collins and Soper was first applied to calculations of the fragmentation functions for heavy quarkonium by Ma [10]. The definition is particularly convenient for carrying out calculations beyond leading order in α_s . It was used by Ma to calculate the short-distance factor of the color-octet 3S_1 term in the gluon fragmentation function to next-to-leading order in α_s [11].

In this paper, we calculate the short-distance coefficients for the color-octet 3S_1 term in the fragmentation function for a gluon to split into heavy quarkonium states to order α_s^2 . We use the gauge-invariant definition of the fragmentation function given by Collins and Soper [1], and we remove ultraviolet divergences using the $\overline{\text{MS}}$ renormalization procedure. Our result for the longitudinal term in the fragmentation function agrees with a previous calculation by Beneke and Rothstein [12]. Our result for the next-to-leading order correction in the transverse term disagrees with a previous calculation by Ma [11].

II. GAUGE-INVARIANT DEFINITION

The fragmentation function $D_{g \rightarrow H}(z, \mu)$ gives the probability that a gluon produced in a hard-scattering process involving momentum transfer of order μ decays into a hadron H carrying a fraction z of the gluon's longitudinal momentum. This function can be defined in terms of the matrix element of a bilocal operator involving two gluon field strengths in a light-cone gauge [9]. In Ref. [1], Collins and Soper introduced a gauge-invariant definition of the gluon fragmentation function that involves the matrix element of a nonlocal operator consisting of two gluon field strengths and eikonal operators. One advantage of this definition is that it avoids subtleties associated with products of singular distributions. The gauge-invariant definition is also advantageous for explicit perturbative calculations, because it allows the calculation of radiative corrections to be simplified by using Feynman gauge.

The gauge-invariant definition of Collins and Soper is

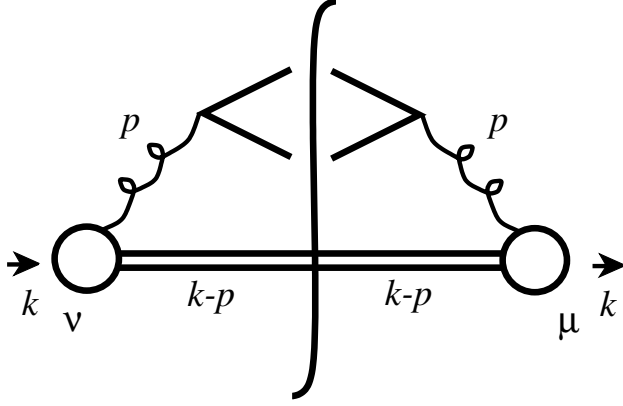


FIG. 1. Leading order Feynman diagram for $g \rightarrow Q\bar{Q}$.

$$D_{g \rightarrow H}(z, \mu) = \frac{(-g_{\mu\nu})z^{N-2}}{16\pi(N-1)k^+} \int_{-\infty}^{+\infty} dx^- e^{-ik^+x^-} \langle 0 | G_c^{+\mu}(0) \mathcal{E}^\dagger(0^-)_{cb} \mathcal{P}_{H(zk^+, 0_\perp)} \mathcal{E}(x^-)_{ba} G_a^{+\nu}(0^+, x^-, 0_\perp) | 0 \rangle. \quad (1)$$

The operator $\mathcal{E}(x^-)$ in (1) is an eikonal operator that involves a path-ordered exponential of gluon field operators along a light-like path:

$$\mathcal{E}(x^-)_{ba} = \text{P exp} \left[+ig \int_{x^-}^{\infty} dz^- A^+(0^+, z^-, 0_\perp) \right]_{ba}, \quad (2)$$

where $A^\mu(x)$ is the matrix-valued gluon field in the adjoint representation: $[A^\mu(x)]_{ac} = if^{abc} A_b^\mu(x)$. The operator $\mathcal{P}_{H(p^+, p_\perp)}$ in (1) is a projection onto states that in the asymptotic future contain a hadron H with momentum $p = (p^+, p^- = (m_H^2 + p_\perp^2)/p^+, p_\perp)$, where m_H is the mass of the hadron. In the definition (1), the hard-scattering scale μ can be identified with the renormalization scale of the nonlocal operator. In perturbative calculations, it is convenient to use dimensional regularization to regularize ultraviolet divergences. The prefactor in the definition (1) has therefore been expressed as a function of the number of spatial dimensions $N = 3 - 2\epsilon$.

For any state H that can be defined in perturbation theory, the definition (1) can be used to calculate the fragmentation function $D_{g \rightarrow H}(z, \mu)$ as a power series in α_s . A convenient set of Feynman rules for this perturbative expansion is given in Ref. [1]. If the state consists of a $Q\bar{Q}$ pair with invariant mass p^2 , the lowest order diagram is shown in Fig. 1. The

circles connected by the double pair of lines represent the nonlocal operator consisting of the gluon field strengths and the eikonal operators. The momentum $k = (k^+, k^-, k_\perp)$ flows into the circle on the left and out the circle on the right. The cutting line represents the projection onto states that in the asymptotic future include a $Q\bar{Q}$ pair with total momentum $p = (zk^+, p^2/(zk^+), 0_\perp)$. If the heavy quark has relative momentum \mathbf{q} in the $Q\bar{Q}$ rest frame, the invariant mass is $p^2 = 4(m_Q^2 + \mathbf{q}^2)$.

The fragmentation of a gluon into heavy quarkonium state H involves many momentum scales, ranging from the hard-scattering scale μ , which we will assume to be larger than m_Q , to momenta much smaller than m_Q where nonperturbative effects are large. The *NRQCD factorization formalism* allows the systematic separation of momentum scales of order m_Q and larger from scales of order $m_Q v$ or smaller, where v is the typical relative velocity of the heavy quark in the hadron. The factorization formula has the form

$$D_{g \rightarrow H}(z, \mu) = \sum_{mn} d_{mn}(z, \mu) \langle \mathcal{O}_{nm}^H \rangle. \quad (3)$$

The *short-distance coefficients* $d_{mn}(z, \mu)$ are independent of the quarkonium state H and can be calculated as a perturbation series in $\alpha_s(m_Q)$. All long-distance effects are factored into the *NRQCD matrix elements* $\langle \mathcal{O}_{nm}^H \rangle$, which can be expressed as matrix elements in an effective field theory. They have the general form

$$\langle \mathcal{O}_{nm}^H \rangle = \langle 0 | \chi^\dagger \mathcal{K}_n \psi \mathcal{P}_H \psi^\dagger \mathcal{K}_m \chi | 0 \rangle, \quad (4)$$

where \mathcal{K}_m and \mathcal{K}_n are constructed out of color matrices, spin matrices, and covariant derivatives and the operator \mathcal{P}_H projects onto states that in the asymptotic future contain a quarkonium state H . The NRQCD matrix elements are nonperturbative but they are universal, with the same matrix elements describing inclusive production in other high energy processes.

The threshold expansion method [13,14] is a general prescription for determining the short-distance coefficients $d_{nm}(z, \mu)$ in the NRQCD factorization formula (3). The diagrams for the fragmentation function of a $Q\bar{Q}$ pair are computed in perturbation theory, except

that the $Q\bar{Q}$ pair is allowed to be in a different state on the two sides of the final-state cut. To the left of the cutting line, the Q and \bar{Q} have relative momentum \mathbf{q} in the $Q\bar{Q}$ rest frame and color and spin states specified by Pauli spinors η and ξ . To the right of the cutting line, the Q and \bar{Q} have relative momentum \mathbf{q}' and color and spin states specified by η' and ξ' . After expanding around the threshold $\mathbf{q} = \mathbf{q}' = 0$, the resulting expression for the diagrams has the form

$$\sum_{mn} d_{mn}(z, \mu) \eta'^{\dagger} \kappa_n \xi' \xi^{\dagger} \kappa_m \eta, \quad (5)$$

where the color and spin matrices κ_m and κ_n are polynomials in the relative momenta \mathbf{q} and \mathbf{q}' . The short-distance coefficients $d_{nm}(z, \mu)$ in the factorization formula (3) can then be read off from this expression. For example, if the sum of the diagrams includes the color-octet 3S_1 terms

$$Nm_Q \left[d_T(z)(\delta^{ij} - \hat{z}^i \hat{z}^j) + d_L(z) \hat{z}^i \hat{z}^j \right] \eta'^{\dagger} \sigma^j T^a \xi' \xi^{\dagger} \sigma^i T^a \eta, \quad (6)$$

then the fragmentation function includes the terms

$$D_{g \rightarrow H}(z) = \frac{N}{4m_Q} \left[d_T(z)(\delta^{ij} - \hat{z}^i \hat{z}^j) + d_L(z) \hat{z}^i \hat{z}^j \right] \langle 0 | \chi^{\dagger} \sigma^j T^a \psi \mathcal{P}_H \psi^{\dagger} \sigma^i T^a \chi | 0 \rangle. \quad (7)$$

If we sum over the spin states of H , the matrix element in (7) is proportional to δ^{ij} and (7) reduces to

$$D_{g \rightarrow H}(z) = [(N-1)d_T(z) + d_L(z)] \langle \mathcal{O}_8^H({}^3S_1) \rangle, \quad (8)$$

where $\langle \mathcal{O}_8^H({}^3S_1) \rangle$ is the color-octet 3S_1 matrix element defined in Ref. [3]:

$$\langle \mathcal{O}_8^H({}^3S_1) \rangle = \frac{1}{4m_Q} \langle 0 | \chi^{\dagger} \sigma^i T^a \psi \mathcal{P}_H \psi^{\dagger} \sigma^i T^a \chi | 0 \rangle. \quad (9)$$

The factor of $1/(4m_Q)$ accounts for the relativistic normalization of the projection operator used in Refs. [13,14].

III. LEADING ORDER

The only Feynman diagram of order α_s for the fragmentation process $g \rightarrow Q\bar{Q}$ is shown in Fig. 1. Using the Feynman rules of Ref. [1], the expression for the diagram can be easily written down in terms of spinors u and v that describe the color, spin, and relative momentum states of the Q and \bar{Q} . We can allow for the Q and \bar{Q} on the right side of the final-state cut to have different color and spin states and different relative momentum \mathbf{q}' by replacing their spinors by u' and v' . The resulting expression is

$$\frac{\pi\alpha_s\mu^{2\epsilon}}{2(N-1)(p^2)^2} \delta(1-z) \left(-g^{\alpha\beta} - \frac{p^2}{(k \cdot n)^2} n^\alpha n^\beta \right) \bar{v}' \gamma_\beta T^a u' \bar{u} \gamma_\alpha T^a v. \quad (10)$$

Setting $\mathbf{q} = \mathbf{q}' = 0$, we can replace the Dirac spinors with Pauli spinors by substituting

$$\bar{u} \gamma_\alpha T^a v = 2m_Q L_{\alpha i} \xi^\dagger \sigma^i T^a \eta, \quad (11)$$

where $L_{\alpha i}$ is a boost matrix that satisfies the identities

$$-g^{\alpha\beta} L_{\alpha i} L_{\beta j} = \delta^{ij}, \quad (12)$$

$$n^\alpha L_{\alpha i} = \frac{p \cdot n}{\sqrt{p^2}} \hat{z}^i. \quad (13)$$

The expression (10) then reduces to

$$\frac{\pi\alpha_s\mu^{2\epsilon}}{8(N-1)m_Q^2} \delta(1-z) (\delta^{ij} - \hat{z}^i \hat{z}^j) \eta'^\dagger \sigma^j T^a \xi' \xi^\dagger \sigma^i T^a \eta. \quad (14)$$

Comparing with (6), we can read off the order- α_s terms in the short-distance functions $d_T(z)$ and $d_L(z)$ defined in (7):

$$d_T^{(\text{LO})}(z) = \frac{\pi\alpha_s\mu^{2\epsilon}}{8N(N-1)m_Q^3} \delta(1-z), \quad (15)$$

$$d_L^{(\text{LO})}(z) = 0. \quad (16)$$

The dependence on the number of spatial dimensions N agrees with that in Ref. [14].

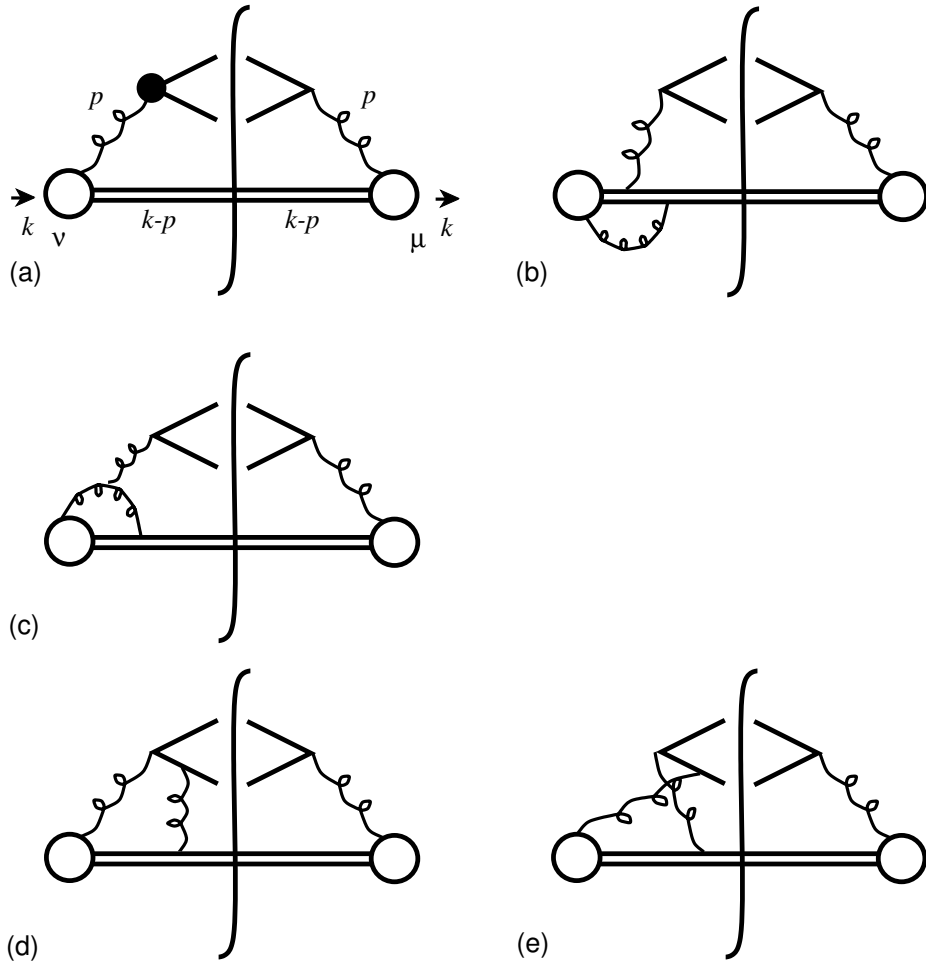


FIG. 2. The Feynman diagrams of order α_s^2 for $g \rightarrow Q\bar{Q}$ with $Q\bar{Q}$ final states. There are additional contributions from the complex-conjugate diagrams.

IV. VIRTUAL CORRECTIONS

The Feynman diagrams for the fragmentation function for $g \rightarrow Q\bar{Q}$ at order α_s^2 consist of virtual corrections, for which the final state is $Q\bar{Q}$, and real-gluon corrections, for which the final state is $Q\bar{Q}g$. The diagrams with virtual-gluon corrections to the left of the cutting line are shown in Fig. 2. The black blob in Fig. 2(a) includes the vertex corrections and propagator corrections shown in Fig. 3.

We calculate the diagrams using Feynman gauge. In this case, the diagram Fig. 2(b) vanishes, because the gluon attaching to the eikonal line gives a factor of n^μ . When con-

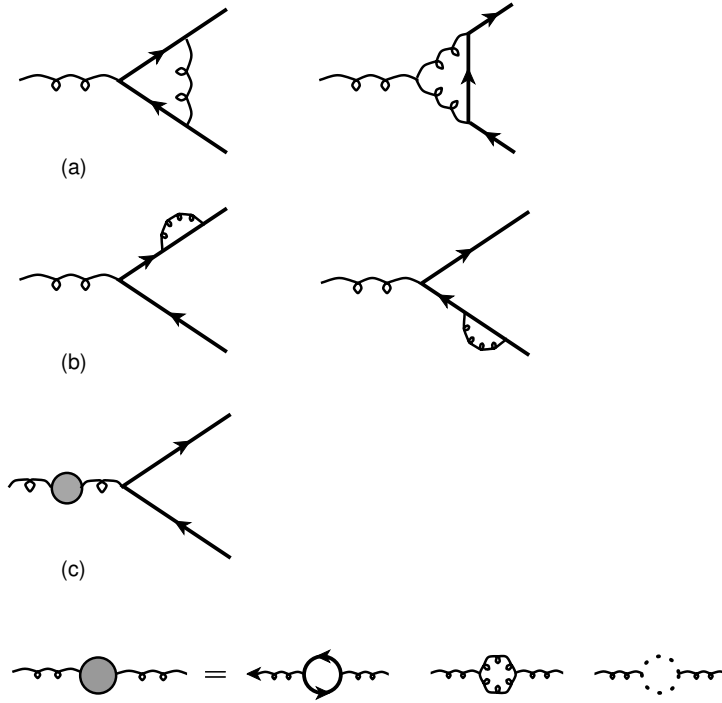


FIG. 3. One loop correction diagrams for $g^* \rightarrow Q\bar{Q}$.

tracted with the factor $k \cdot n g^{\nu\beta} - p^\nu n^\beta$ from the circle on the left side of the cut, it gives a factor $(k - p) \cdot n = 0$. In the limit $\mathbf{q} = \mathbf{q}' = 0$, all the other diagrams can be reduced to the leading order diagram in Fig. 1 times a multiplicative factor. For the diagrams in Fig. 2(a), this follows from the Dirac equation for the heavy-quark spinors. For the remaining diagrams, we must also use the fact that the contraction of n^μ with the right side of the diagram vanishes.

The virtual corrections contribute only to the transverse short-distance function $d_T(z)$ defined in (7). We will express the various contributions in the form of the leading-order result (15) times a multiplicative factor. The sum of the diagrams in Fig. 2(a), together with their complex conjugates, is

$$d_T^{(2a)}(z) = d_T^{(\text{LO})}(z) \times 2 \operatorname{Re} \left[\Lambda + \Pi + (Z_Q - 1) \right], \quad (17)$$

where Λ is the vertex correction factor from the diagrams in Fig. 3(b), Π is the propagator correction factor for a gluon with invariant mass $4m_Q^2$ from the diagrams in Fig. 3(d), and

$Z_Q - 1$ comes from the wavefunction renormalization factors $Z_Q^{1/2}$ for the heavy quark from the diagrams in Fig. 3(c). These correction factors are given by

$$\Lambda = \frac{\alpha_s}{\pi} \left(\frac{\pi\mu^2}{m_Q^2} \right)^\epsilon \left[\frac{13}{12} \frac{\Gamma(1+\epsilon)}{\epsilon_{UV}} - \frac{1}{12} \frac{\Gamma(1+\epsilon)}{\epsilon_{IR}} + \frac{13}{6} + 3 \ln 2 - i \frac{\pi}{2} \right], \quad (18)$$

$$Z_Q - 1 = \frac{\alpha_s}{\pi} \left(\frac{\pi\mu^2}{m_Q^2} \right)^\epsilon \left[-\frac{1}{3} \frac{\Gamma(1+\epsilon)}{\epsilon_{UV}} - \frac{2}{3} \frac{\Gamma(1+\epsilon)}{\epsilon_{IR}} - \frac{4}{3} - 2 \ln 2 \right], \quad (19)$$

$$\Pi = \frac{\alpha_s}{\pi} \left(\frac{\pi\mu^2}{m_Q^2} e^{i\pi} \right)^\epsilon \left[\frac{15 - 2n_f}{12} \frac{\Gamma(1+\epsilon)}{\epsilon_{UV}} + \frac{93 - 10n_f}{36} \right], \quad (20)$$

where n_f is the number of light quark flavors. The subscripts on the poles in ϵ indicate whether the divergences are of ultraviolet or infrared origin. The sum of the virtual corrections given in (17) is

$$d_T^{(2a)}(z) = d_T^{(LO)}(z) \times \frac{\alpha_s}{\pi} \left(\frac{\pi\mu^2}{m_Q^2} \right)^\epsilon \Gamma(1+\epsilon) \left[\frac{12 - n_f}{3\epsilon_{UV}} - \frac{3}{2\epsilon_{IR}} + \frac{123 - 10n_f}{18} + 2 \ln 2 \right], \quad (21)$$

Ma's result for these diagrams [11] differs by an additive constant -5.487 inside the square brackets and by setting $N(N-1) \rightarrow 3(N-1)$ in $d_T^{(LO)}(z)$.

The contribution from the diagrams in Fig. 2(c) with its complex conjugate is

$$d_T^{(2c)}(z) = d_T^{(LO)}(z) \times 24\pi\alpha_s\mu^{2\epsilon} \operatorname{Re} \left[i(2k \cdot n I_{ABC} - I_{AB}) \right], \quad (22)$$

where the scalar integrals $I_{AB\dots}$ are given in appendix A. The contribution from the sum of the diagrams in Figs. 2(d) and 2(e) with their complex conjugates is

$$d_T^{(2d,e)}(z) = d_T^{(LO)}(z) \times 96\pi\alpha_s\mu^{2\epsilon}m_Q^2 \operatorname{Re} \left[i(k \cdot n I_{ABCD} - I_{ABD}) \right]. \quad (23)$$

The sum of the virtual corrections given in (22) and (23) is

$$d_T^{(2c,d,e)}(z) = d_T^{(LO)}(z) \times \frac{\alpha_s}{\pi} \left(\frac{\pi\mu^2}{m_Q^2} \right)^\epsilon \Gamma(1+\epsilon) \left[\frac{3(1-\epsilon)}{2\epsilon_{UV}\epsilon_{IR}} + \frac{3}{2\epsilon_{UV}} + 3 - \frac{\pi^2}{2} + 6 \ln 2 + 6 \ln^2 2 \right]. \quad (24)$$

Ma's result for these diagrams [11] differs by an additive constant $-3 + \frac{3}{2}\pi^2 - 6 \ln^2 2$ inside the square brackets and by setting $N(N-1) \rightarrow 3(N-1)$ in $d_T^{(LO)}(z)$.

The total virtual correction is the sum of (21) and (24):

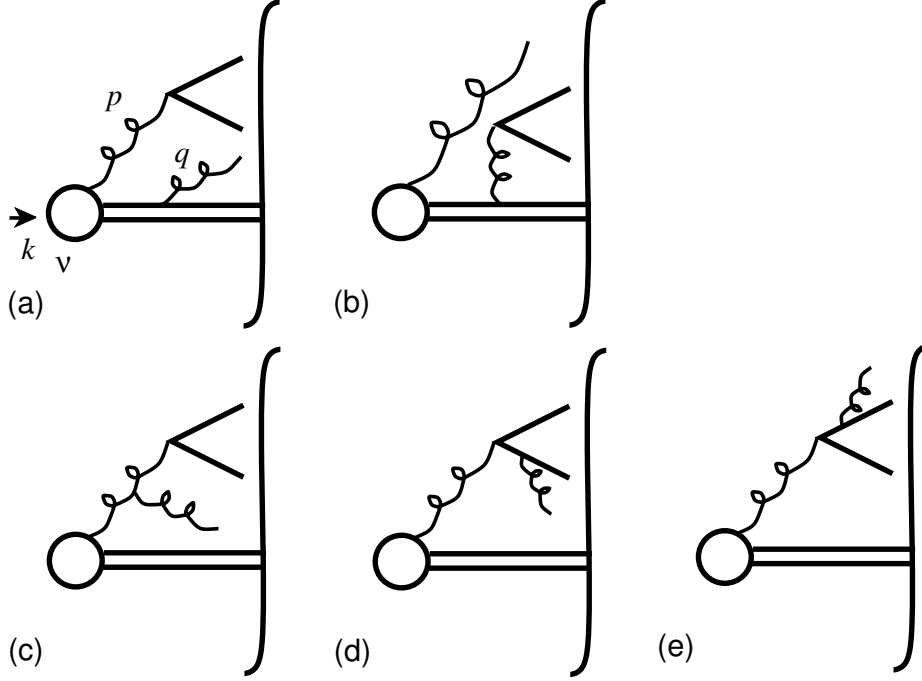


FIG. 4. The Feynman diagrams of order α_s^2 for $g \rightarrow Q\bar{Q}$ with $Q\bar{Q}g$ final states. There are a total of 25 diagrams, but only the left halves of the diagrams are shown.

$$d_T^{(\text{virtual})}(z) = d_T^{(\text{LO})}(z) \times \frac{\alpha_s}{\pi} \left(\frac{\pi\mu^2}{m_Q^2} \right)^\epsilon \left[\frac{3(1-\epsilon)\Gamma(1+\epsilon)}{2\epsilon_{UV}\epsilon_{IR}} + \beta_0 \frac{\Gamma(1+\epsilon)}{\epsilon_{UV}} + \frac{177-10n_f}{18} - \frac{\pi^2}{2} + 8\ln 2 + 6\ln^2 2 \right], \quad (25)$$

where $\beta_0 = (33 - 2n_f)/6$.

V. REAL GLUON CORRECTIONS

The Feynman diagrams for the real-gluon corrections to the fragmentation function for $g \rightarrow Q\bar{Q}$ pair are shown in Fig. 4. We draw the 5 left-half diagrams only, but they must be multiplied by their complex conjugates to give a total of 25 diagrams. Only diagrams 4(a), 4(b) and 4(c) contribute to the color-octet 3S_1 term, which reduces the total number of diagrams to 9. We calculate the diagrams using Feynman gauge. After a considerable amount of algebra, they reduce to

$$d_T^{(\text{real})}(z) = \frac{\pi\alpha_s\mu^{2\epsilon}}{8N(N-1)m_Q^3} \times \frac{3\alpha_s}{\pi\Gamma(1-\epsilon)} \left(\frac{\pi\mu^2}{m_Q^2}\right)^\epsilon \left(1 - \frac{1}{z(1-z)}\right)^2 \int_{(1-z)/z}^\infty dx \frac{t^{1-\epsilon}}{x^2}, \quad (26)$$

$$d_L^{(\text{real})}(z) = \frac{\pi\alpha_s\mu^{2\epsilon}}{8Nm_Q^3} \times \frac{3\alpha_s}{\pi\Gamma(1-\epsilon)} \left(\frac{\pi\mu^2}{m_Q^2}\right)^\epsilon \left(\frac{1-z}{z}\right)^2 \int_{(1-z)/z}^\infty dx \frac{t^{-\epsilon}}{x^2}, \quad (27)$$

where $t = (1-z)(zx+z-1)$, $x = 2q \cdot p/p^2$, q is the final-state gluon momentum, and p is the $Q\bar{Q}$ momentum. Integration over x can be done using the following identities:

$$\int_{(1-z)/z}^\infty dx \frac{t^{1-\epsilon}}{x^2} = z(1-z)^{1-2\epsilon} \frac{1-\epsilon}{\epsilon_{UV}} B(1+\epsilon, 1-\epsilon), \quad (28)$$

$$\int_{(1-z)/z}^\infty dx \frac{t^{-\epsilon}}{x^2} = z(1-z)^{-1-2\epsilon} B(1+\epsilon, 1-\epsilon). \quad (29)$$

The subscript on ϵ in (28) indicates that the pole has an ultraviolet origin. In (26), there is also an infrared divergence associated with the limit $z \rightarrow 1$. It can be made explicit by using the expansion:

$$\frac{1}{(1-z)^{1+2\epsilon}} = -\frac{1}{2\epsilon_{IR}}\delta(1-z) + \frac{1}{(1-z)_+} - 2\epsilon \left(\frac{\ln(1-z)}{1-z}\right)_+ + O(\epsilon^2). \quad (30)$$

The final results for the real-gluon corrections are

$$d_T^{(\text{real})}(z) = \frac{\pi\alpha_s\mu^{2\epsilon}}{8N(N-1)m_Q^3} \times \frac{\alpha_s}{\pi} \left(\frac{\pi\mu^2}{m_Q^2}\right)^\epsilon \Gamma(1+\epsilon) \left[-\frac{3(1-\epsilon)}{2\epsilon_{UV}\epsilon_{IR}}\delta(1-z) + \frac{3(1-\epsilon)}{\epsilon_{UV}} \left(\frac{z}{(1-z)_+} + \frac{1-z}{z} + z(1-z)\right) - \frac{6}{z} \left(\frac{\ln(1-z)}{1-z}\right)_+ + 6(2-z+z^2)\ln(1-z) \right], \quad (31)$$

$$d_L^{(\text{real})}(z) = \frac{\pi\alpha_s}{8Nm_Q^3} \times \frac{3\alpha_s}{\pi} \frac{1-z}{z}. \quad (32)$$

Note that the double-pole term proportional to $1/(\epsilon_{UV}\epsilon_{IR})$ in (31) exactly cancels its counterpart in the virtual correction (25). The sum of (25) and (31) is free of infrared divergences. Ma's result for the real-gluon corrections [11] is completely different from the sum of (31) and (32). In particular, he found that the $[\ln(1-z)/(1-z)]_+$ terms cancelled. In the way we organized the calculation, there is no possibility of such a cancellation.

VI. RENORMALIZATION

The sum of the order- α_s^2 corrections to $d_T(z)$ in (25) and (31) still contains ultraviolet divergences in the form of single poles in ϵ . These divergences are cancelled by the renormalization of the coupling constant α_s in the leading-order expression (16) and by the renormalization of the nonlocal operator in (1). The renormalization of α_s in the $\overline{\text{MS}}$ scheme can be carried out by making the following substitution in (16):

$$\alpha_s \rightarrow \alpha_s \left[1 - \frac{\alpha_s}{2\pi} \beta_0 (4\pi e^{-\gamma})^\epsilon \frac{1}{\epsilon_{UV}} \right], \quad (33)$$

where $\beta_0 = (33 - 2n_f)/6$. The operator renormalization in the $\overline{\text{MS}}$ scheme can be carried out by making the following substitution

$$d_T^{(\text{LO})}(z) \rightarrow d_T^{(\text{LO})}(z) - \frac{\alpha_s}{2\pi} (4\pi e^{-\gamma})^\epsilon \frac{1}{\epsilon_{UV}} \int_z^1 \frac{dy}{y} P_{gg}(y) d_T^{(\text{LO})}(z/y), \quad (34)$$

where $P_{gg}(y)$ is the gluon splitting function:

$$P_{gg}(z) = 6 \left[\frac{z}{(1-z)_+} + \frac{1-z}{z} + z(1-z) + \frac{\beta_0}{6} \delta(1-z) \right]. \quad (35)$$

The sum of the two contributions of order α_s^2 from renormalization is

$$\begin{aligned} d_T^{(\text{ren})}(z) &= \frac{\pi \alpha_s \mu^{2\epsilon}}{8N(N-1)m_Q^3} \\ &\times \frac{\alpha_s}{\pi} (4\pi e^{-\gamma})^\epsilon \frac{(-3)}{\epsilon_{UV}} \left[\frac{z}{(1-z)_+} + \frac{1-z}{z} + z(1-z) + \frac{\beta_0}{3} \delta(1-z) \right]. \end{aligned} \quad (36)$$

This cancels the single ultraviolet poles in the sum of (25) and (31). Our final result for the transverse fragmentation function is obtained by adding the order- α_s^2 corrections to $d_T(z)$ from (25), (31), and (36) and taking $\epsilon \rightarrow 0$:

$$\begin{aligned} d_T(z, \mu) &= \frac{\pi \alpha_s(\mu)}{48m_Q^3} \left\{ \delta(1-z) + \frac{\alpha_s(\mu)}{\pi} \left[A(\mu) \delta(1-z) + \left(\ln \frac{\mu}{2m_Q} - \frac{1}{2} \right) P_{gg}(z) \right. \right. \\ &\quad \left. \left. + 6(2-z+z^2) \ln(1-z) - \frac{6}{z} \left(\frac{\ln(1-z)}{1-z} \right)_+ \right] \right\}, \end{aligned} \quad (37)$$

where the coefficient $A(\mu)$ is

$$A(\mu) = \beta_0 \left(\ln \frac{\mu}{2m_Q} + \frac{13}{6} \right) + \frac{2}{3} - \frac{\pi^2}{2} + 8 \ln 2 + 6 \ln^2 2. \quad (38)$$

The result (37) disagrees with the final result obtained by Ma [11]. Our final result for the longitudinal fragmentation function is obtained by setting $\epsilon \rightarrow 0$ in (32):

$$d_L(z, \mu) = \frac{\alpha_s^2(\mu)}{8m_Q^3} \frac{1-z}{z}. \quad (39)$$

This agrees with the result of Beneke and Rothstein [12]. The fragmentation probabilities obtained by integrating $d_T(z)$ and $d_L(z)$ diverge, because these functions behave like $1/z$ as $z \rightarrow 0$. The higher moments of the fragmentation functions however are well-defined.

VII. DISCUSSION

The color-octet 3S_1 term in the fragmentation function is important for calculating the production at large p_T of spin-singlet S-wave states, like the J/ψ , and spin-triplet P-wave states, like the χ_{cJ} . We can deduce the fragmentation functions for each of their spin states by using the approximate spin symmetry of NRQCD to simplify the expression (7). The functions $d_T(z)$ in (37) and $d_L(z)$ (39) give the fragmentation functions for the transverse and longitudinal spin states of the J/ψ , respectively:

$$D_{g \rightarrow J/\psi(\pm 1)}(z) = d_T(z) \langle \mathcal{O}_8^{J/\psi}({}^3S_1) \rangle, \quad (40)$$

$$D_{g \rightarrow J/\psi(0)}(z) = d_L(z) \langle \mathcal{O}_8^{J/\psi}({}^3S_1) \rangle. \quad (41)$$

The sum over spin states is

$$D_{g \rightarrow J/\psi}(z) = [2d_T(z) + d_L(z)] \langle \mathcal{O}_8^{J/\psi}({}^3S_1) \rangle. \quad (42)$$

The fragmentation functions for each of the spin states of the χ_{cJ} are [16]

$$D_{g \rightarrow \chi_{c0}}(z) = [2d_T(z) + d_L(z)] \langle \mathcal{O}_8^{\chi_{c0}}({}^3S_1) \rangle, \quad (43)$$

$$D_{g \rightarrow \chi_{c1}(0)}(z) = 3d_T(z) \langle \mathcal{O}_8^{\chi_{c1}}({}^3S_1) \rangle, \quad (44)$$

$$D_{g \rightarrow \chi_{c1}(\pm 1)}(z) = \frac{3}{2} [d_T(z) + d_L(z)] \langle \mathcal{O}_8^{\chi_{c1}}({}^3S_1) \rangle, \quad (45)$$

$$D_{g \rightarrow \chi_{c2}(0)}(z) = [d_T(z) + 2d_L(z)] \langle \mathcal{O}_8^{\chi_{c0}}(^3S_1) \rangle, \quad (46)$$

$$D_{g \rightarrow \chi_{c2}(\pm 1)}(z) = \frac{3}{2} [d_T(z) + d_L(z)] \langle \mathcal{O}_8^{\chi_{c0}}(^3S_1) \rangle, \quad (47)$$

$$D_{g \rightarrow \chi_{c2}(\pm 2)}(z) = 3d_T(z) \langle \mathcal{O}_8^{\chi_{c0}}(^3S_1) \rangle. \quad (48)$$

The sums over spin states are

$$D_{g \rightarrow \chi_{cJ}}(z) = (2J + 1) [2d_T(z) + d_L(z)] \langle \mathcal{O}_8^{\chi_{c0}}(^3S_1) \rangle. \quad (49)$$

In order to give accurate predictions for the production of quarkonium at large p_T , it is important to know the next-to-leading order correction to the color-octet 3S_1 term in the gluon fragmentation function. Unfortunately our calculation of the short-distance coefficient disagrees with the previous calculation by Ma. An independent calculation of this important function is therefore essential.

This work was supported in part by the U.S. Department of Energy Division of High Energy Physics under grant DE-FG02-91-ER40690, by the Alexander von Humboldt Foundation, and by the Korea Institute for Advanced Study. J.L. would like to thank the OSU theory group for its hospitality during his stay in Columbus.

APPENDIX A: INTEGRAL TABLE

In this appendix, we present the explicit values of the integrals encountered in evaluating the virtual-gluon corrections. These integrals have the form

$$I_{AB\dots} = \int \frac{d^{N+1}l}{(2\pi)^{N+1}} \frac{1}{AB\dots}, \quad (A1)$$

where the denominator $AB\dots$ can be a product of 1, 2, 3, or 4 of the following factors:

$$A = l^2 + i\epsilon, \quad (A2)$$

$$B = (l - p)^2 + i\epsilon = l^2 - 2l \cdot p + 4m_Q^2 + i\epsilon, \quad (A3)$$

$$C = (p - l) \cdot n + i\epsilon, \quad (A4)$$

$$D = (l - p/2)^2 - m_Q^2 + i\epsilon = l^2 - l \cdot p + i\epsilon. \quad (A5)$$

The momentum p is that of a $Q\bar{Q}$ pair with zero relative momentum ($p^2 = 4m_Q^2$) and n is light-like ($n^2 = 0$). The integrals I_A and I_B vanish in dimensional regularization. By symmetry under $p \rightarrow l - p$, we have $I_{AD} = I_{BD}$. Some of the integrals can be reduced to ones with fewer denominators by using the identity $A + B - 2D = 4m_Q^2$:

$$4m_Q^2 I_{ABD} = 2(I_{AD} - I_{AB}), \quad (\text{A6})$$

$$4m_Q^2 I_{ABCD} = I_{ACD} + I_{BCD} - 2I_{ABC}. \quad (\text{A7})$$

The independent integrals that need to be evaluated are therefore

$$I_{AB} = \frac{i}{(4\pi)^2} \left(\frac{\pi e^{i\pi}}{m_Q^2} \right)^\epsilon \frac{\Gamma(1+\epsilon)\Gamma^2(1-\epsilon)}{\epsilon_{UV}\Gamma(2-2\epsilon)}, \quad (\text{A8})$$

$$I_{AD} = \frac{i}{(4\pi)^2} \left(\frac{4\pi}{m_Q^2} \right)^\epsilon \frac{\Gamma(1+\epsilon)}{\epsilon_{UV}(1-2\epsilon)}, \quad (\text{A9})$$

$$I_{ABC} = \frac{-i}{(4\pi)^2 p \cdot n} \left(\frac{\pi e^{i\pi}}{m_Q^2} \right)^\epsilon \frac{\Gamma(1+\epsilon)\Gamma^2(1-\epsilon)}{\epsilon_{UV}\epsilon_{IR}\Gamma(1-2\epsilon)}, \quad (\text{A10})$$

$$I_{ACD} = \frac{+i}{(4\pi)^2 p \cdot n} \left(\frac{4\pi}{m_Q^2} \right)^\epsilon \frac{\Gamma(1+\epsilon)}{\epsilon_{UV}} \left[2 \ln 2 + \epsilon \left(\frac{\pi^2}{3} - 6 \ln^2 2 \right) + O(\epsilon^2) \right], \quad (\text{A11})$$

$$I_{BCD} = \frac{-i}{(4\pi)^2 p \cdot n} \left(\frac{4\pi}{m_Q^2} \right)^\epsilon \frac{\Gamma(1+\epsilon)}{\epsilon_{UV}\epsilon_{IR}}. \quad (\text{A12})$$

The subscripts on the poles in ϵ indicate whether the divergences are of ultraviolet or infrared origin.

REFERENCES

- [1] J.C. Collins and D.E. Soper, Nucl. Phys. B **193**, 381 (1981); *ibid.* B **194**, 445 (1982).
- [2] E. Braaten and T.C. Yuan, Phys. Rev. Lett. **71**, 1673 (1993); Phys. Rev. D **52**, 6627 (1995).
- [3] G.T. Bodwin, E. Braaten, and G.P. Lepage, Phys. Rev. D **51**, 1125 (1995).
- [4] E. Braaten and T.C. Yuan, Phys. Rev. D **50**, 3176 (1994);
- [5] E. Braaten and S. Fleming, Phys. Rev. Lett. **74**, 3327 (1995).
- [6] P. Cho and M.B. Wise, Phys. Lett. **B346**, 129 (1995).
- [7] E. Braaten, Kingman Cheung, and T.C. Yuan, Phys. Rev. D **48**, 4230 (1993).
- [8] E. Braaten, Kingman Cheung, and T.C. Yuan, Phys. Rev. D **48**, R5049 (1993).
- [9] G. Curci, W. Furmanski, and R. Petronzio, Nucl. Phys. **B175**, 27 (1980).
- [10] J.P. Ma, Phys.Lett. **B 332**, 398 (1994).
- [11] J.P. Ma, Nucl. Phys. B **447**, 405 (1995).
- [12] M. Beneke and I.Z. Rothstein, Phys. Lett. B **372**, 157 (1996); (E):*ibid.* B **389**, 769 (1996).
- [13] E. Braaten, Y.-Q. Chen, Phys. Rev. D **54**, 3216 (1996).
- [14] E. Braaten, Y.-Q. Chen, Phys. Rev. D **55**, 2693 (1997).
- [15] E. Braaten, Y.-Q. Chen, Phys. Rev. D **55**, 7152 (1997).
- [16] P. Cho, M.B. Wise, and S.P. Trivedi, Phys. Rev. D **51**, 2039 (1995).